

Investigation of the friction and wear properties of nitrided 7075-T6 aluminum alloy under vacuum and ambient air

Nitrürlenmiş 7075-T6 alüminyum alaşımının vakum ve atmosfer şartlarında sürtünme ve aşınma özelliklerinin incelenmesi

Hojjat GHAHRAMANZADEH ASL¹ , Yaşar SERT^{1*} , Özgü BAYRAK² , Tevfik KÜÇÜKÖMEROĞLU¹ 

¹Department of Engineering Mechanical, Engineering Faculty, Karadeniz Technical University, Trabzon, Turkey.
h.kahramanzade@ktu.edu.tr, yasarsert@ktu.edu.tr, tkomer@ktu.edu.tr

²Department of Biomedical Engineering, Engineering Faculty, Izmir Bakırçay University, Izmir, Turkey.
ozgu.bayrak@bakircay.edu.tr

Received/Geliş Tarihi: 25.01.2021
Accepted/Kabul Tarihi: 29.06.2021

Revision/Düzeltilme Tarihi: 28.06.2021

doi: 10.5505/pajes.2021.83903
Research Article/Araştırma Makalesi

Abstract

Al7075 alloy is commonly used in the automotive industry, components of military vehicles and aircraft, rubber and plastic moulds. Also, similar Al alloys are frequently used for mechanical parts in space exploration. Therefore, investigation of the wear properties under a vacuum environment is as indispensable as wear properties under an atmosphere. However, the wear performance of this alloy cannot meet the expectations. This paper reports the investigation of the obtained wear properties of Al7075-T6 alloy after plasma nitriding in ambient air and vacuum environments. The surface characterization and phase analysis of the formed AlN layers are determined by scanning electron microscope, energy dispersive X-ray spectrometer, 3D optical profilometer and X-ray diffractometer. The hardness of the nitride layer is established using Vickers micro-hardness tester. The wear performance of the untreated and nitride sample is investigated under 1N constant load at ambient air and vacuum environment. As a result of wear tests, the best wear performance of both conditions has been obtained from nitrided samples. The AlN layer (0.19) is observed to notably reduced the coefficient of friction of the substrate (0.60) under ambient air. Besides, it is observed that the nitride layer is better in ambient air (0.00010 mm³/Nm) than in vacuum environment (0.00087 mm³/Nm) in term of wear rate. In fact, the wear track on the nitrided sample is very thin under ambient air, and nearly imperceptible.

Keywords: Al7075-T6, Plasma Nitriding, Wear, Vacuum.

Öz

Al7075 alaşımları, otomotiv endüstrisinde, askeri araçların ve uçakların bileşenlerinde, kauçuk ve plastik kalıplarda yaygın olarak kullanılmaktadır. Ayrıca, benzer Al alaşımları, uzay araştırmalarında mekanik parçalar için sıklıkla kullanılmaktadır. Bu nedenle, vakum altında aşınma özelliklerinin incelenmesi, atmosfer ortamındaki aşınma özellikleri kadar vazgeçilmezdir. Ancak söz konusu alaşımların aşınma performansı beklentileri karşılamamaktadır. Bu bağlamda, bu çalışmada nitrürlenmiş Al7075-T6'nın atmosfer ve vakum ortamlarında aşınma özelliklerinin belirlenmesi amaçlanmıştır. Oluşturulan AlN tabakasının yüzey karakterizasyonu ve faz analizi, taramalı elektron mikroskobu, enerji dağıtıcı X-ışını spektrometresi, 3D optik profilometre ve X-ışını difraktometresi ile belirlenmiştir. Numunelerin sertliği, Vickers mikro sertlik test cihazı kullanılarak belirlenmiştir. Numunelerin aşınma performansı, bilye disk esaslı aşınma test cihazı kullanılarak atmosfer ve vakum ortamlarında incelenmiştir. Her iki koşul için de en iyi aşınma performansı nitrürlenmiş numunelerden elde edilmiştir. AlN tabakasının (0,19), ortam havası altında alt tabakanın (0,60) sürtünme katsayısını önemli ölçüde azalttığı gözlemlenmiştir. Nitrür tabakası sayesinde, alaşımın atmosfer ortamındaki aşınma direnci dikkate değer bir şekilde iyileştirilmiştir. Ayrıca aşınma oranı açısından nitrür tabakasının aşınma performansı, ortam havasında (0.00010 mm³/Nm) vakum ortamına (0.00087 mm³/Nm) göre daha iyi olduğu gözlemlenmiştir. Hatta numunelerdeki aşınma yolunun çok ince olduğu ve neredeyse fark edilemez olduğu gözlemlenmiştir.

Anahtar kelimeler: Al7075-T6, Plazma nitrüleme, Aşınma, Vakum.

1 Introduction

It is a known fact that Al alloys have widespread use as structural materials, especially in aerospace, manufacturing and architectural fields, thanks to their high mechanical strength to weight ratio and favourable formability [1],[4]. Although Al alloys are widely used, they also have some limitation, such as poor wear resistance application fields [5]. Wear is the most important phenomenon that causes mechanical systems in contact with each other to be damaged and become unusable [6],[7]. It should be considered that improving the performance of the mechanical components in spacecraft where Al alloys are widely used today will contribute to future space research. Especially, the working sensitivity of the satellites sent to space for reasons such as communication

technologies, military purposes is very high. It is very important to prevent damage, as component replacement in space is very difficult. Therefore, compared to the wear occurring in any industrial application, the wear seen in space equipment such as satellites causes more economical and social negativity. Due to these economic and scientific reasons, it is quite clear that the wear resistance of Al alloys should be enhanced [8],[9]. Therefore, considering the developments in materials science, first, there are studies to improve the mentioned properties of Al alloys by changing the microstructure, which is the oldest technique known. Heat treatment is a very critical phenomenon for these microstructure alteration [10],[11]. However, aluminum alloys are divided into two main groups as forging and casting alloys, depending on the manufacturing method. Aluminum alloys produced by forging have numerous

*Corresponding author/Yazışılan Yazar

advantages compared to cast aluminum, such as excellent mechanical properties, ease of forming and structural integrity etc. That is why, this study will focus on aluminum alloys produced by forging. The alloys in these two groups can be examined in subgroups as heat treated, and non-heat treated alloys. According to the Aluminum Association, wrought aluminum alloys are classified by four numbers, with the first number from 1 to 8. Among these alloys, 2XXX, 6XXX, 7XXX and 8XXX series can be hardened by heat treatment. Al 7075 has become an attractive material, especially in space and aviation industry, due to its lightness and high strength properties considering the other hardenable Al alloys [12],[13]. In Al7075, which is a Cu-based Al-Zn alloy, Mg, Cr and Zr are additional alloying elements. In 7075 alloys produced by adding 4-8% Zn and 1-3% Mg to Al, both Zn and Mg have high solid solubility and these reinforcements generally provide high precipitation hardening. However, the addition of 2% Cu to these alloys also enhances their mechanical properties and helps them to stand out using in aircraft and spacecraft parts [14]. Studies and research continue day by day within the scope of developing material properties in the world of science. In this context, there has been a tremendous increase in the studies using different processes to further improve the strength and wear properties of the 7075 alloys. The most known and used of these processes is the heat treatment, which includes precipitation hardening carried out after solution, quenching and ageing [15],[16]. It consists of the dissolving of the phases in the solution process, the forming of a supersaturated structure in the quenching process, and the precipitation of solute atoms at room or elevated temperatures in the aging process [17]. The whole processes consist of the following phase transformation stages.

Supersaturated solid solution \longrightarrow Guinier Preston (GP) zones
 \longrightarrow η (MgZn₂) \longrightarrow η (MgZn₂)

Composed of the supersaturated solid solution, GP (Guinier-Preston) zones are compatible with the matrix and unstable. While GP zones can be occurred by ageing at room temperature, the common application in the literature is artificial ageing in the temperature range of 100-180 °C [18]. In the Al-Zn-Mg alloy system, the interface energy for the GP zones is very low. The low interface contributes to the increase of the density of these tiny zones in the structure. The η phase, defined as a metastable, has a monoclinic unit cell. The η (MgZn₂) phase, which is stable, has a hexagonal close-packed (HCP) crystal structure [19]. The basic logic of this heat treatment process which is called T6 is that the nanometer-sized MgZn₂ strengthening particles precipitate in the matrix during ageing and ensure the high value of hardness and mechanical properties of the alloys [19]. The importance of heat treatment in improving the usage performance of the Al alloys is stated above. When regarding the advances in surface engineering in recent years, it is confident that the surface treatments performed to heat-treated Al alloys will add a new perspective to the solution of the wear-related drawbacks. Moreover, the above efforts will be in vain for solving the wear problems in these competitive conditions of the developing industry, unless taken innovative approaches to the surface treatments. For this goal, the Al₂O₃ layer is formed on the surface of Al alloy employing anodizing or other plasma-assisted techniques [2]. However, as stated by Zhao, Al₂O₃ has low thermal conductivity [20]. Especially for this reason, it is exposed to severe adhesion property in metal-ceramic contact. This negative behavior of the Al₂O₃ encountered on the contact surfaces has shifted the

research to other surface treatment methods. Some research emphasized the treating of the surface to considerably increase the friction and wear performance via plasma nitriding for Al alloys [21]. Thanks to the nitriding process, the AlN layer formed on the Al alloy surface is remarkable due to its high wear resistance, electrical resistivity, and thermal conductivity [5],[22]. On the other hand, during the nitriding process of the Al alloys, attention should be paid not to form an Al₂O₃ layer on the surface. Because if Al₂O₃ is formed on the Al surface, which is very sensitive to oxygen, this stable and hard layer will have a negative effect that prevents the diffusion of nitrogen atoms. In order to avoid this limitation, as stated by Stock, the Al₂O₃ layer is removed by sputtering H₂ as a pretreatment before the diffusion of nitrogen [23]. After this pretreatment, the nucleation process is started, and AlN nodules and islands are formed on the surface [5]. When the surface of the alloy is completely covered with these islands, finally, the nitrogen diffusion process is carried out in a controlled manner and the AlN is formed on the surface. With the day by day advancement of vacuum technology, the necessity of the pretreatment performed to prevent the oxide layer in the nitriding process has disappeared. Fitz emphasized the need for good vacuum conditions, i.e. low oxygen pressure associated with ion energy and current density, for the perfection of the nitriding process [24]. In this direction, the nitriding process is performed at 10⁻⁶ Pa high-level vacuum conditions in this study and the nitrogen diffusion problem caused by the oxygen sensitivity of Al alloys was minimized. It has been determined that the temperature is effective up to which AlN phases formed. Manova et al. indicated that F.C.C AlN is encountered at 300 °C or below [24]. Furthermore, it is expected that the temperature of the substrate plays a very important role as nitriding is essentially a diffusion process [25]. In the related study, this effect of temperature is explained as the rearrangement of the h-AlN preferential phase by increasing the mobility of Al atoms at high temperature. On the other hand, Fitz encountered the c-AlN phase in the nitriding process performed at elevated temperatures [25]. It was emphasized above that nitriding is essentially a diffusion process. Also, it has been revealed in the open literature that the diffusion mechanism is related to the growth of the nitride layer on the surface. During the nitriding process, nitride layer grows due to the dominant diffusion from the underlying agglomerates towards the surface where a new AlN is formed.

As it is the main purpose of the study, it is clearly emphasized that the Al7075-T6 alloy with a higher wear performance than other Al alloys, it's widely used in the space industry. Therefore, it would be more meaningful to concentrate on improving the wear performance of the Al7075-T6 rather than bringing the wear properties of an Al alloys such as 2XXX and 6XXX series with lower wear properties to Al7075-T6 levels. Since the subject is based on to further improve the wear performance of Al 7075-T6 spacecraft components with nitriding process, tribological investigation in an atmosphere-free vacuum environment is quite essential. However, as a result of the literature survey, it has not been encountered that the wear behavior of nitrided Al7075-T6 alloy in a vacuum environment has been investigated satisfactorily. Therefore, in this study, the wear performance of nitrided Al7075-T6 alloy in a vacuum environment was examined in comparison with the untreated alloy. The wear tests of the nitrided alloy were carried out using computer-controlled ball-on disc tribometer. Then, a scanning electron microscope (SEM) and energy dispersive

spectrometer (EDS) were employed for characterization of the wear mechanism and elemental analysis of the wear tracks. Also, a micro-hardness tester and XRD were employed to determine the mechanical properties and structural phases of samples.

2 Experimental details

2.1 Sample preparations

The chemical composition of Al 7075-T6 alloy is given in Table 1.

Table 1. Chemical composition of Al7075-T6.

Element	Mg	Si	Fe	Cu	Mn	Zn	Cr	Al
wt. %	2.5	0.4	0.5	1.6	0.25	5.7	0.22	Bal.

The Al 7075-T6 samples, which have 25x25x5 mm³ in dimension were used as a substrate material in this study. Samples were ground by using 400, 800, 1200, 2000, 4000 mesh SiC papers to eliminate any unwanted defects and protrusions during the cutting process. Then samples were polished with 1 µm Al₂O₃ solution. After cleaning with ethanol, samples were dried and made ready for the plasma nitriding process.

2.2 Plasma nitriding process

The plasma nitriding chamber was evacuated to 1x10⁻⁶ Pa pressure then, H₂ was filled into the chamber until the pressure reaches 6.66 Pa (50 mtorr) for the sputtering process. The samples were heated up to the specified temperature by a heater, and a sputtering process performed for 15 min. After this process, the chamber was once more evacuated to 1x10⁻⁶ Pa. Nitriding process was performed using a RF plasma nitriding setup at 400 °C temperature for 1 h. All specimens were treated under the same condition, which was 80 vol.% nitrogen and 20 vol.% argon mixture atmosphere, 100 V potential and 6.66 Pa (50 mtorr) pressure.

2.3 Characterization of samples

The phase analysis of the nitrided Al 7075 alloy was characterized using Bragg-Brentano mode X-Ray diffractometer (XRD, Panalytical Empyrean, United Kingdom) with λ = 1.5405 Å and Cu Kα radiation at 3 deg/min. scan speed, 10-100 deg. scan range and 0.005 deg. scan step operation parameters. Scanning electron microscope (SEM, FEI Quanta, EFG 450, USA) was employed to investigate the microstructure of the nitrided sample. The chemical compositions of the samples were determined by an energy dispersive spectrometer (EDS). Besides, the roughness of surfaces was examined with an optical profilometer (Nanofocus, µscan Custom, Germany). Hardness measurements of samples were performed using Vickers type micro-hardness tester (Struers Duramin, Denmark). These measurements were carried out five times for each sample under 10 g constant load with 10 seconds dwell time. The tribo-tests were conducted by computer-controlled DUCOM (TR-201V, India) according to ASTM G 99-17 standards suitable for performing high vacuum environment. During the experiments, the coefficient of friction (COF) was recorded automatically. Two different counter bodies as 6 mm diameter WC and Al₂O₃, were used for abrader. These tests were performed under high vacuum (0.001 Pa) and ambient air (room temperature). During the wear tests, the counter bodies were stationary and the lower disc has a rotating speed of 60 mm/s. The diameter of wear track was set

up as 8 mm. Also, 1 N constant load was chosen for tests. The topography of the wear tracks and the worn volume of the samples were determined by an optical profilometer (Nanofocus, µscan Custom, Germany) with 2 µm x 2 µm resolution. By using the measured worn volume value, in the Archard formula which was given in formula (1), the wear rate of samples was calculated.

$$W = V / (P * D) \quad (1)$$

In related formula; “W”: wear rate (mm³/Nm), “V”: wear volume (mm³), “P”: constant load (N) and “d”: sliding distance (m). SEM (Zeiss EVO LS10, Germany) was used to characterize the wear mechanisms of all samples and counter bodies. Also, line-EDS analysis was carried out from the inside and outside of the wear tracks for elemental investigations.

3 Results and discussion

3.1 Morphology and microstructures

Figure 1 shows the surface of the nitrided sample. The particles formed on the surface of sample are nitrides. This shows that a coating consisting of aluminum nitride particles has been formed on the aluminum substrate. Also, it was observed that the nitride surfaces have a very dense structure. According to Taherkhani et al. after the nitriding process, a particulate appearance will be obtained on the surface of the material [26].

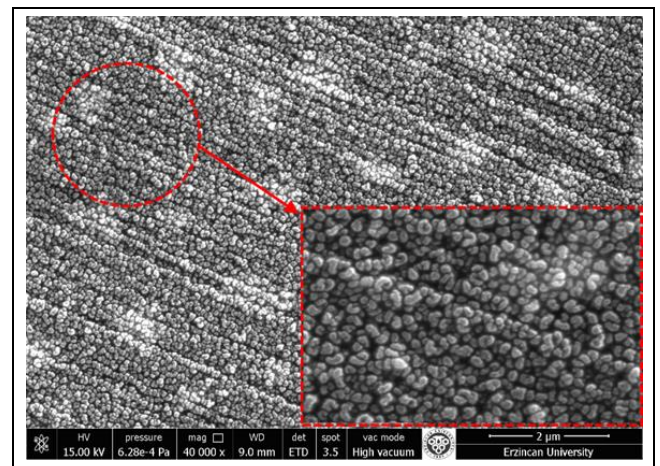


Figure 1. SEM images of the nitrided sample surface

The average surface roughness of the untreated and nitrided samples are shown in Figure 2.

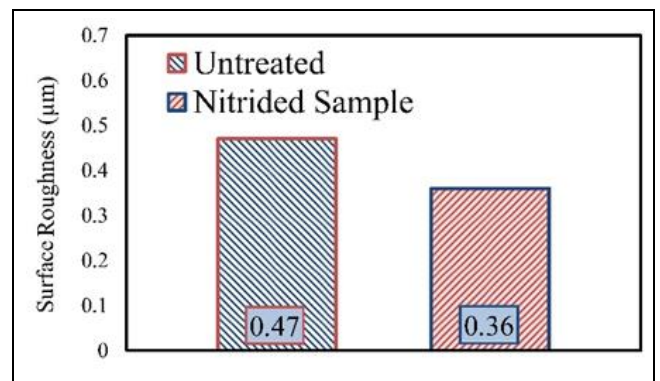


Figure 2. Surface roughness of untreated and nitrided samples.

After the surface preparation, the roughness of surface was attained as 0.47 μm for the untreated sample. After the nitriding process, the roughness was decreased $\sim 28\%$. Apparently, the surface roughness has decreased due to the ion scattering on the aluminum surface during the plasma treatment and the filling of the valleys formed because of the mechanical preparation. According to Visuttipitukul et al. the surface roughness plays an important role in the homogeneous formation of AlN. Also, they emphasized that AlN formation gives better results if the surface roughness values of the samples are below 1 μm [2].

3.2 EDS and XRD analysis

Chemical compositions of untreated and nitrided sample are given in Table 2. Additionally, XRD patterns of untreated and nitrided sample are shown in Figure 3.

Table 2. Surface chemical composition of untreated and nitrided sample (wt%).

Element	Untreated	Nitrided
	Weight %	Weight %
Al	98.77	84.62
Fe	1.23	1.18
N	-----	14.20

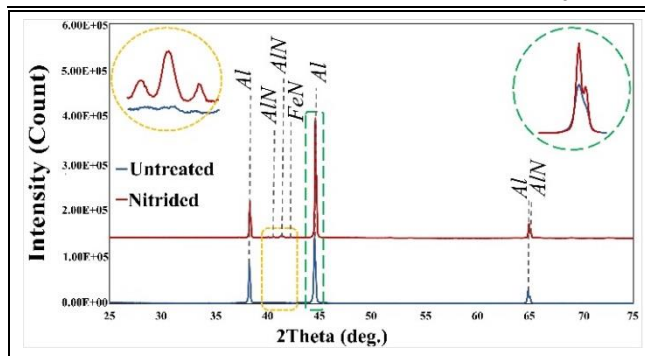


Figure 3. X-ray patterns of untreated and nitrided sample.

Examination of EDS results given in Table 1, yielded that the amount of nitrogen on the surfaces of the nitrided sample was increased and the amount of aluminum was decreased. Besides, iron (Fe) was found on the untreated and nitrided sample surfaces. After the nitriding process, it was determined that the Fe content changed slightly, while the Al decreased significantly. This situation is related to fresh phases in XRD with enhance in the quantity of nitrogen diffusing to samples surface. The nitrided sample exhibited various nitride formations, as seen in the XRD graph. Besides, aluminum oxide phase is not encountered on untreated and nitrided samples. This refers that the aforementioned phase was very low in amount or very thin to be determined by XRD analysis. The essential nitride phase on the nitrided sample was AlN. These results reveal that the oxygen was removed from the environment by creating a vacuum and the aluminum oxide phase was not formed. In addition to the AlN phase formation, it was seen that the FeN phase was formed. Also, Al peaks were seen in the nitrided sample. According to Taherkhani et al.'s study, the presence of the Al phase in the coated samples should be attributed to the very low thickness of the coating. This allows X-rays to pass and reach the aluminum substrate. Although some of this Al phase may belong to the coating itself, this is unlikely as aluminum is highly reactive to nitrogen and rapidly converts to AlN upon exposure to this element [26]. According to Taherkhani et al. and Vissuttipitukul et al. it was

concluded that the nitride layer formed in the plasma nitriding of Al 7075 alloy have F.C.C structure with high strength. In addition, it was stated in these studies that F.C.C.-AlN has a high volumetric density [27],[28].

The nitrided sample was cut by precision cutting after it was moulded into bakelite. After the metallographic preparation of the cross-section, EDS analysis was carried out from 12 different points up to the depth of approximately 10 μm , as given in Figure 4. In this way, the diffusion depth of the nitrogen to the surface was also determined. As seen in the EDS analysis, a decrease in the amount of nitrogen was detected as it moved away from the surface to the inwards of the sample. In addition to the excess nitrogen just below the sample surface, it was seen that there is $\sim 6\%$ at a depth of about 9 μm . Based on the data, it can be inferred that the nitrogen diffusion depth in the sample is approximately 10 μm .

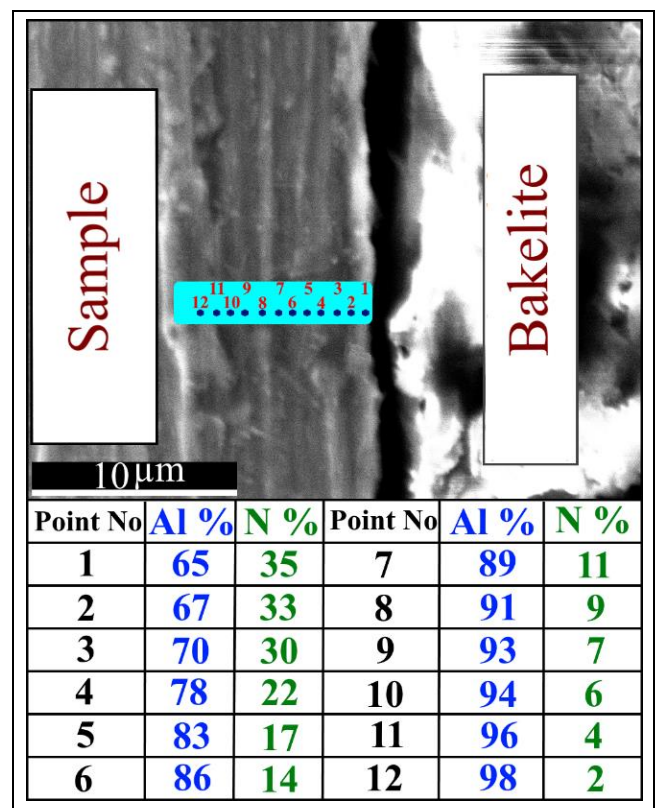


Figure 4. Point EDS analysis of nitrided sample.

3.3 Micro-hardness

Micro-hardness values of samples are seen in Figure 5. The hardness value of the untreated Al7075-T6 alloy was determined as $\sim 215 \pm 8$ HV_{0.01}. Then, the hardness was measured by removing the nitride layer on the surface of the nitrided sample. However, after the nitriding process, it was found that the micro-hardness value decreased in the substrate. It was determined that the hardness of the sample with the nitride layer removed was $\sim 72 \pm 5$ HV_{0.01}. Looking at the literature, it was seen that the hardness value of the Al7075-T6 alloy was 195-215 HV [14]. The hardness value has decreased since the nitriding process was applied at 400 °C. The reason for this was that the effects of T6 treatment disappear, in other words, the material was annealed at this temperature. In the literature, the hardness value of Al7075 alloy without T6 treatment has been reported as ~ 71 HV [29].

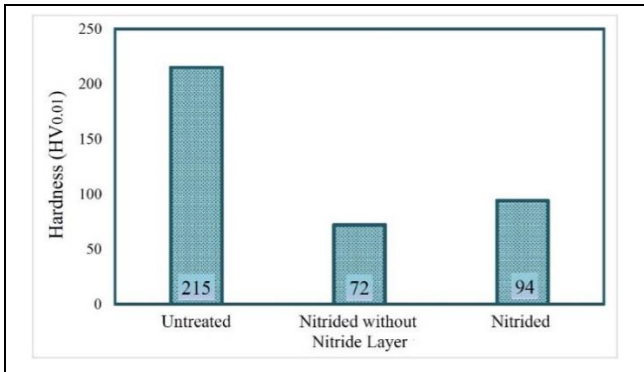


Figure 5. Microhardness of Al7075 Alloy before and after plasma nitride.

The values we have obtained are utterly compatible with the literature. In addition, Panigrahi et al. stated in their study that the hardness values of Al7075-T6 alloy decreased as a result of annealing at 400 °C for 1 hour from ~190 HV to ~98 HV [30]. In the present study, an increase in the hardness was observed in the nitrided sample in comparison with the sample with the removed nitride layer. The hardness value was obtained as ~94 HV in the nitrided sample. The main reason for the low hardness of the nitride layer was the decrease in hardness of the substrate. As it is known, the thin film layer present on the surface of the material is affected by the load-bearing capacity of the base material in micro-hardness analysis. Therefore, the cross-sectional hardness measurement was performed on the sample and given in Figure 6. The hardness value at the closest point that can be taken under the surface was measured as ~138 HV_{0.01}. It was detected that this value decreased from the surface of the sample to inwards. The substrate hardness was reached at a depth of ~10-15 µm. This finding was coherent with the point EDS results taken from the cross-section.

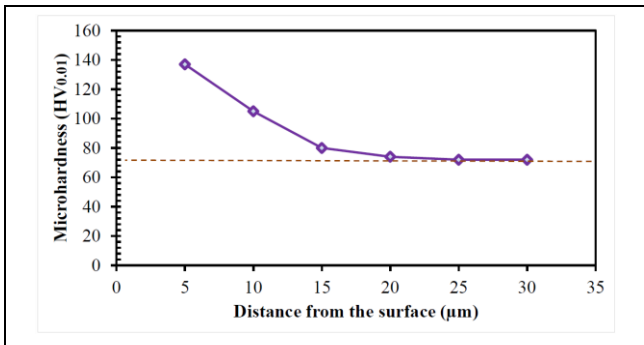


Figure 6. The cross-sectional hardness value of nitrided sample.

3.4 Coefficient of Friction and wear behavior

Figure 7 shows the coefficient of friction with respect to cycle under vacuum and ambient air conditions for the wear tests. In addition, the coefficient of friction values are given in Table 3. At the beginning of the tests, all samples show a rapid increase in the friction coefficient due to Hertzian contact [31],[32]. Subsequently, the friction coefficients achieve stability in different durations, regimes, and values. Regarding the untreated samples, alumina counter body under vacuum and ambient air conditions show very similar behaviors. An only slight increase was observed after ~1400 cycles in ambient air. This may be caused by the oxidized wear particles getting stuck between the mating surfaces [33]. Coefficient of friction (COF)

values of WC ball under ambient air and vacuum conditions exhibit different characteristics. COF under ambient air seemed to reach a steady state faster, and it was lower in value. Apparently, relative humidity favours the friction by acting as a lubricating agent [34].

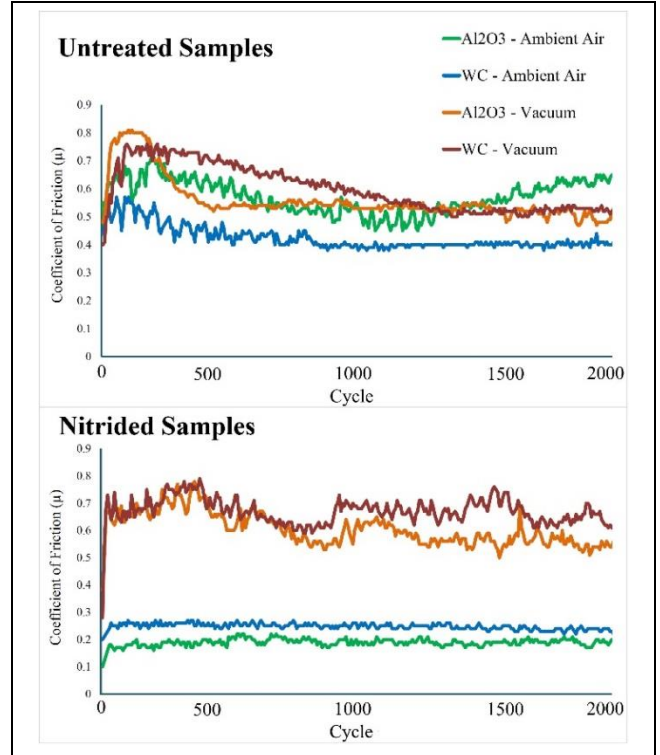


Figure 7. The coefficient of friction-cycle graphics of untreated and nitrided sample under vacuum and ambient air conditions with different counter body.

Table 3. The coefficient of friction values of samples.

Test Group	Untreated Samples			
	Al ₂ O ₃ - Ambient Air	WC- Ambient Air	Al ₂ O ₃ - Vacuum	WC- Vacuum
Friction Coefficient	0.6	0.42	0.58	0.55
Test Group	Nitrided Samples			
	Al ₂ O ₃ - Ambient Air	WC- Ambient Air	Al ₂ O ₃ - Vacuum	WC- Vacuum
Friction Coefficient	0.19	0.25	0.6	0.69

The difference between ambient air and vacuum conditions became more pronounced for nitrided samples. COF values and behavior of WC and Alumina counter bodies under vacuum condition were very similar. COFs were even slightly higher than the untreated samples under same condition which is usually expected because of the stronger adhesion of surface atoms under vacuum condition. Surprisingly, the nitrided samples showed very favourable COF values under ambient air. The fact that samples with the same process parameters performed poorly under vacuum condition indicates that low COFs cannot be attributed solely to the surface nitride layer. An interaction between the surface nitride phases and relative humidity appears to play a role in these conditions via adsorption of a gas film [34].

The optical profilometer images of the wear tracks are shown in Figure 8. Wear track widths of untreated samples in ambient air were significantly wider than all the others. On the other hand, wear tracks of nitrided samples in ambient air were almost nonexistent. This result also supports the fact that very low friction coefficients were obtained in these samples. Wear rate calculations were performed using optic profilometer images and the calculated values of untreated and nitrided samples are given in Figure 9. There seems to be no apparent correlation between COF values and wear rates of untreated samples. WC in ambient air showed the highest wear rate in contrast with its friction coefficient. Alumina in ambient air also exhibited high wear rate. However, although the adhesion between surfaces increases under vacuum, the wear rates of the samples are lower. This can be attributed to the oxidation of the wear particles and their formation of hard abrasive bodies in the ambient air. Such particles plough through the wear path and increase the worn volume [35].

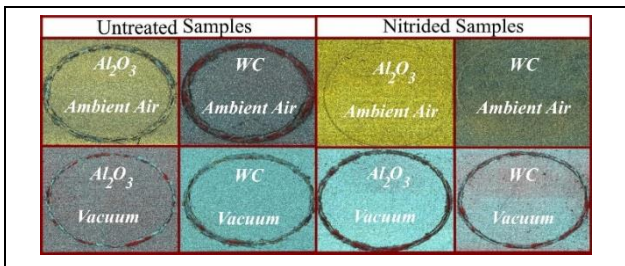


Figure 8. Optical profilometer images of wear tracks.

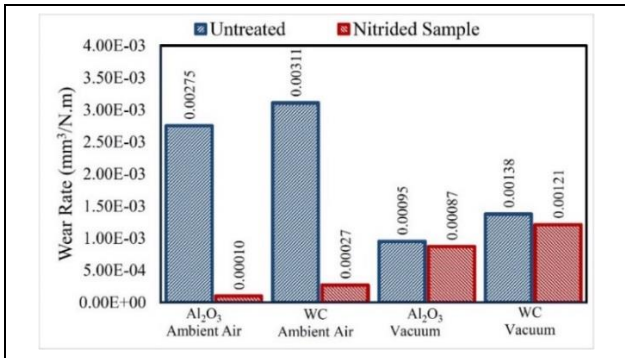
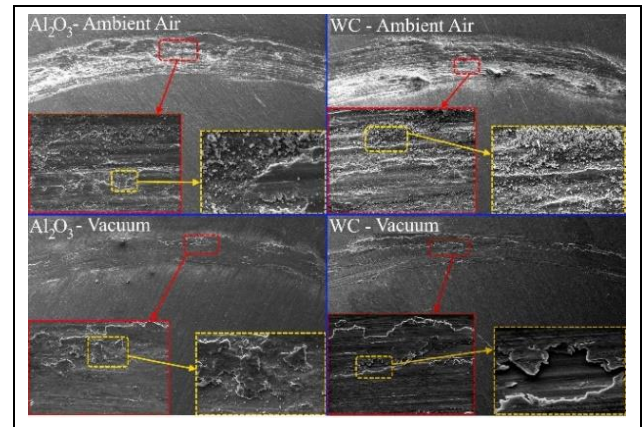


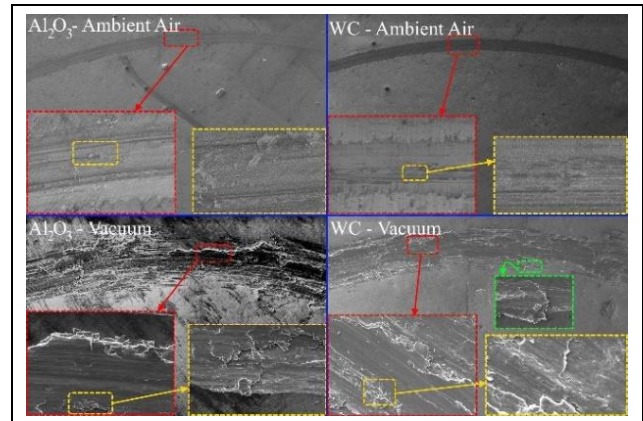
Figure 9. Wear rate values of samples under vacuum and ambient air conditions.

When the nitrided specimens are examined, it can be seen that the samples with low COF also yield low wear rates, but once again, no direct correlation could be made. For instance, while nitrided specimen tested with WC under ambient air had the lowest COF, the wear rate of the same condition was slightly higher than the sample tested with Al₂O₃. Similarly, samples under vacuum condition showed close wear rate values. What should be noted was the fact that untreated and nitrided samples displayed almost identical wear rates under vacuum. It is known in scientific literature that adhesion between mating surfaces is largely dependent on oxygen pressure in vacuum and it decreases as oxygen pressure increases [36]. Another important finding was that the experiments with the WC wear ball showed higher wear rates than counterparts made with the alumina wear ball. This may be due to the fact that the WC ball is a metal matrix carbide ceramic composite, whereas the alumina ball is an oxide ceramic. Therefore, the interaction between the contact surfaces differentiates at atomic level.

Another important implication of all the results is that surface or bulk hardness is not the only factor determining the wear rate. Although hardness is defined as the resistance to plastic deformation, the amount of wear that occurs depends on many reasons, such as the interaction of surface atoms in contact, the cohesion of surface atoms, oxidation of wear products or transfer film formation. The worn surfaces formed after the wear test under vacuum, and ambient air condition are investigated employing SEM and corresponding images are seen in Figure 10. Besides, the wear magnitude was given in Table 4.



(a)



(b)

Figure 10. SEM images of wear tracks of (a): Untreated and (b): Plasma nitrided samples under vacuum and ambient air conditions.

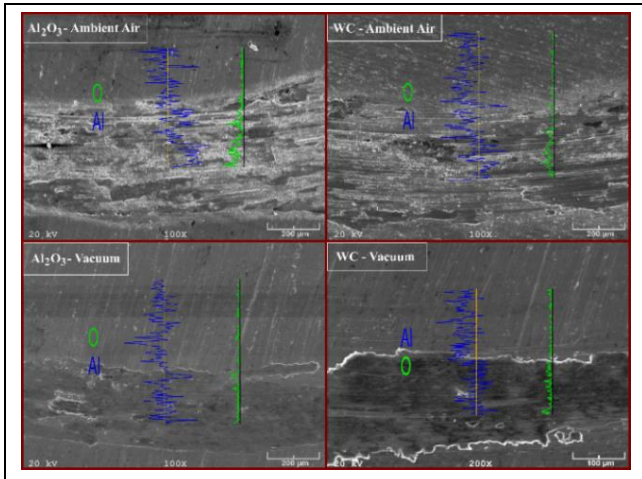
Table 4. Wear magnitude of samples.

Test Group	Untreated Samples			
	Al ₂ O ₃ - Ambient Air	WC- Ambient Air	Al ₂ O ₃ - Vacuum	WC- Vacuum
Wear Magnitude (µm)	520	600	260	325
Test Group	Nitrided Samples			
	Al ₂ O ₃ - Ambient Air	WC- Ambient Air	Al ₂ O ₃ - Vacuum	WC- Vacuum
Wear Magnitude (µm)	85	130	190	295

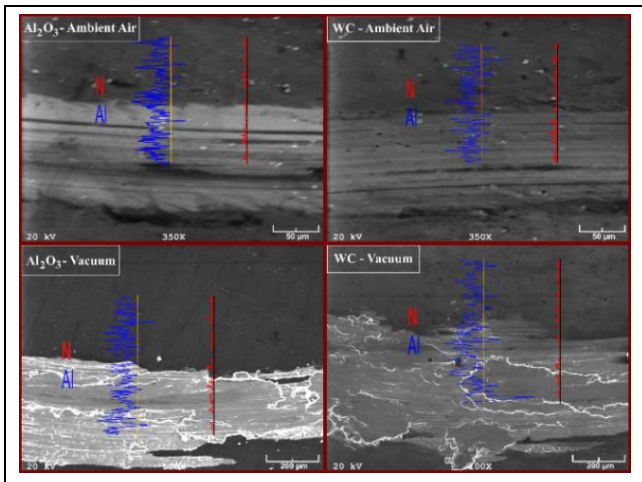
Fine wear particles could be observed on untreated samples tested under ambient air. For both wear ball, the wear mechanism seems to start as adhesive. Plastically deformed

and probably deformation hardened parts of the surface started oxidizing with the help of the friction heat and chipped off from the surface, creating third body abrasive particles [37]. After this, the mechanism has turned into abrasive wear, creating grooving marks along the wear tracks. Under vacuum condition, however, the abrasive wear particles were not present. Therefore, the governing wear mechanism remained as adhesive. Plastic flow promoted subsurface cracks that were parallel to the surface. These cracks were then reached the surface, and delaminated pieces forming platelet-like wear particles [38].

When nitrided specimens worn under ambient air were examined, it was seen that the hardened surface resisted deforming plastically with the help of the lubricating effect of the absorbed gas film due to relative humidity, and the wear was mostly achieved by a polishing-like mechanism where the surface roughness was flattened. The nitrided samples showed higher level of plastic deformation under vacuum. Once again, mostly adhesive wear with cracked and delaminated platelet-like structures which resembling galling was observed due to the lack of humidity [39],[40]. The linear EDS analysis of the worn surface of samples is given in Figure 11.



(a)

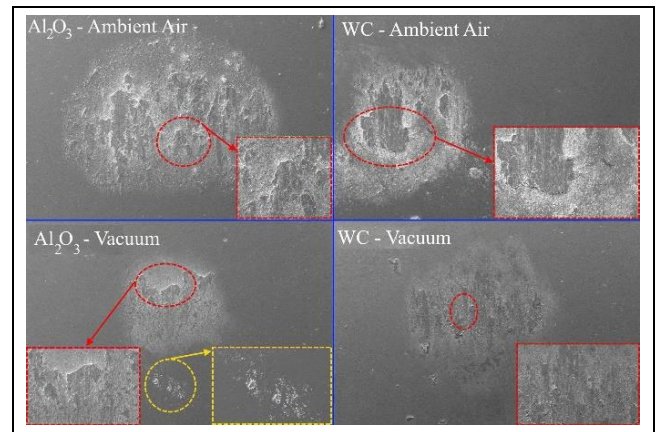


(b)

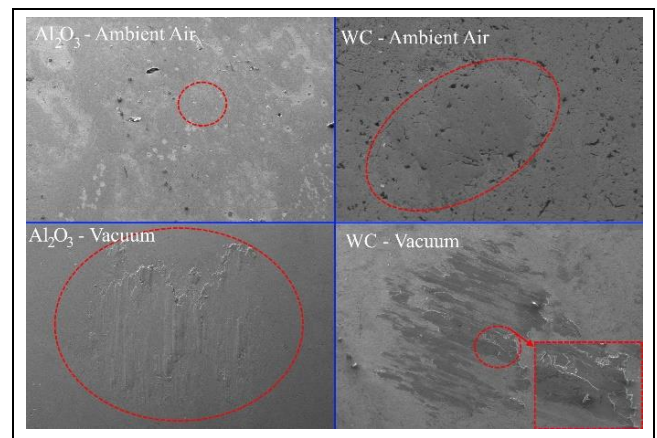
Figure 11. EDS analysis of wear tracks of (a): Untreated and (b): Plasma nitrided samples under vacuum and ambient air conditions.

For the untreated samples, the oxygen content increased within the wear path. This is in conjunction with our discussions about the wear mechanism regarding these samples. In the plasma nitrided samples, there was no significant change in the nitrogen amount inside and outside the wear path. Accordingly, it can be concluded that the difference in wear rates and coefficients of friction is independent of nitrogen content, but is related to the changing surface chemistry with the presence of nitrogen and relative humidity.

The SEM images of the surface of counter bodies are shown in Figure 12 for all samples. Among the untreated samples, it was seen that the largest wear trace was on the alumina ball tested in ambient air condition. In addition, abrasive oxide particles and parallel grooves could be seen in both Al₂O₃ and WC balls. In the tests performed in a vacuum condition, there was a decrease in the contact area. It could be said that a transfer film was formed under all conditions of the untreated samples, but that this film was broken to form hard oxide particles in ambient air and plate structures under vacuum. In nitrided samples, on the other hand, in the experiments conducted in ambient air, almost no wear marks were seen on the wear pins. Thus, there was no oxide particles or transfer film formation. In experiments under vacuum, wear products transferred on the pin can be seen. This confirmed that under vacuum, a strong adhesion bond between the pin and the surface occurred despite the nitride layer.



(a)



(b)

Figure 12. SEM images of counter body surfaces of (a): Untreated and (b): Plasma nitrided samples under vacuum and ambient air conditions

4 Conclusions

In this study, plasma nitriding at 400 °C was performed on Al7075-T6 under vacuum environment. Wear resistance properties of nitride Al7075 alloys under vacuum and ambient air environments were examined. The results obtained from this paper are given below.

- Owing to the high vacuum created in the environment during nitriding process, Al₂O₃ phase was not encountered in the structure,
- It should be noted as a success that the structure does not oxidize at the high temperatures reached in the nitriding process of the Al alloys,
- On the surface of the Al7075-T6 after plasma nitriding, AlN and FeN phases were formed,
- The depth of the nitrogen diffusion was determined to be approximately 10 µm
- In the nitriding process, the T6 temper properties of the Al 7075 alloy has disappeared, so a decrease in the hardness of the substrate has occurred. However, the hardness values in the diffusion zone are higher than the substrate,
- It was observed that the wear rate was lower in nitrided samples than the untreated samples. However, this difference was more pronounced in the ambient air,
- It was observed that the dominant wear mechanism in the ambient air condition of the untreated samples was abrasive with third body, but the adhesive wear mechanism was more dominant in the vacuum environment,
- All in all, Al7075 that was treated with plasma nitriding technique, could raise life and application areas of the Al7075-T6 components. This situation is certain to cause serious enhancement in the service life of this kind of alloy, especially in areas of use where wear is more important than strength.

5 Author contribution statements

In the scope of this study, the Hojjat GHARAMANZADEH ASL and Özgü BAYRAK in the formation of the idea, the design and the literature review; Yaşar SERT in the assessment of obtained results, supplying the materials used and examining the results; the Tevfik KÜÇÜKÖMEROĞLU the spelling and checking the article in terms of content were contributed.

6 Ethics committee approval and conflict of interest statement

There is no need to obtain permission from the ethics committee for the article prepared.

There is no conflict of interest with any person / institution in the article prepared.

7 References

- [1] Kaseem M, Lee Y H, Ko Y G. "Incorporation of MoO₂ and ZrO₂ particles into the oxide film formed on 7075 Al alloy via micro-arc oxidation". *Materials Letters*, 182, 260-263, 2016.
- [2] Visuttipitukul P, Aizawa T. "Plasma nitriding design for aluminium and aluminium alloys". *Surface Engineering*, 22(3), 187-195, 2006.
- [3] Totik Y, Sadeler R, Kaymaz I, Gavgali M. "The effect of homogenisation treatment on cold deformations of AA 2014 and AA 6063 Alloys". *Journal of Materials Processing Technology*, 147(1), 60-64, 2004.
- [4] Taskin M, Caligulu U, Gur A K. "Modeling adhesive wear resistance of Al-Si-Mg-/SiCp PM compacts fabricated by hot pressing process, by means of ANN". *The International Journal of Advanced Manufacturing Technology*, 7, 715-721, 2008.
- [5] Visuttipitukul P, Aizawa T, Kuwahara H. "Advanced plasma nitriding for aluminum and aluminum alloys". *Materials Transactions*, 44(12), 2695-2700, 2003.
- [6] Kara L, Özkan D, Yağcı M B, Sulukan E, Sert Y, Sert T S. "Friction and wear behaviors of TiN coating under dry and vacuum conditions". *Tribology Transactions*, 62(3), 362-373, 2019.
- [7] Gavgali M, Totik Y, Sadeler R. "The effects of artificial aging on wear properties of AA 6063 alloy". *Materials Letters*, 57(24-25), 3713-3721, 2003.
- [8] Abdelgnei MA, Omar MZ, Ghazali MJ, Mohammed MN, Rashid B. "Dry sliding wear behaviour of thixoformed Al-5.7Si-2Cu-0.3 Mg alloys at high temperatures using taguchi method". *Wear*, 442-443, 203134, 2020.
- [9] Shaik M A, Golla B R. "Development of highly wear resistant cu-al alloys processed via powder metallurgy". *Tribology International*, 136, 127-139, 2019.
- [10] Isadare AD, Aremo B, Adeoye MO, Olawale OJ, Shittu MD. "Effect of heat treatment on some mechanical properties of 7075 aluminium alloy". *Materials Research*, 16(1), 190-194, 2013.
- [11] Mahathaninwong N, Plookphol T, Wannasin J, Wisutmethangoon S. "T6 heat treatment of rheocasting 7075 Al alloy". *Materials Science and Engineering: A*, 532, 91-99, 2012.
- [12] Şimşek I, Yıldırım M, Özyürek D, Tunçay T. "The effect of aging time on wear behaviours of aa7075 alloy in t6 heat treatment". *Journal of Advanced Technology Sciences*, 7(1), 42-49, 2018.
- [13] Imran M, Khan A R A. "Characterization of Al-7075 metal matrix composites: a review". *Journal of Materials Research and Technology*, 8(3), 3347-3356, 2019.
- [14] Yıldırım M, Şimşek İ, Özyürek D. "An investigation of the effects of solid solution temperature on the wear performance of aged aa7075 alloy". *Gazi Üniversitesi Fen Bilimleri Dergisi Part C: Tasarım ve Teknoloji*, 6(1), 233-239, 2018.
- [15] Ravi Kumar DV, Seenappa, Ravi Kumar V, Prakash Rao CR. "Influence of T6-Heat treatment on mechanical properties of Al7075 alloy reinforced with cenosphere". *Materials Today: Proceedings*, 5(11), 25036-25044, 2018.
- [16] Yavuz S, Sert Y, Karşlı M, Küçükömeroğlu T. "Determining optimum anodic oxidation parameters for hardness and wear properties of AA7075-T6 alloys using taguchi desing". *Brilliant Engineering*, 1, 10-18, 2021.
- [17] Zhao Y H, Liao X Z, Zhu Y T, Valiev R Z. "Enhanced mechanical properties in ultrafine grained 7075 Al alloy". *Journal of Materials Research*, 20(2), 288-291, 2005.
- [18] Fakioglu A, Özyürek D. "Effects of re-aging on the fatigue properties of aluminium alloy AA7075". *Materials Testing*, 56(7-8), 575-582, 2014.

- [19] Komra Y, Tokunaga K. "Structural studies of stacking variants in mg-base friauf-laves phases". *Acta Crystallographica Section B: Structural Crystallography and Crystal Chemistry*, 16(7), 1548-1554, 1980.
- [20] Zhao Z W, Tay B K, Sheeja D. "Structural characteristics and mechanical properties of aluminium oxide thin films prepared by off-plane filtered cathodic vacuum arc system". *Surface and Coatings Technology*, 167(2-3), 234-239, 2003.
- [21] Aizawa T, Vissutipitukul P. "Formation of aluminum nitrides by precipitate-accommodated plasma nitriding". *MRS Proceedings*, 1040, 809, 2007. <https://doi.org/10.1557/PROC-1040-Q08-09>
- [22] Chen H-Y, Stock H-R, Mayr P. "Plasma-Assisted nitriding of aluminium and its alloys". *Surface and Coatings Technology*, 64, 139-147, 1994.
- [23] Stock H R, Jarms C, Seidel F, Döring J E. "Fundamental and applied aspects of the plasma-assisted nitriding process for aluminium and its alloys". *Surface and Coatings Technology*, 94-95, 247-254, 1997.
- [24] Manova D, Huber P, Mändl S, Rauschenbach B. "Surface modification of aluminium by plasma immersion ion implantation". *Surface and Coatings Technology*, 128-129, 249-255, 2000.
- [25] Fitz T. "Ion Nitriding of Aluminium". *Forschungszentrum Rossendorf*, Dresden, Technische Universität Dresden 2002.
- [26] Taherkhani K, Soltanieh M. "Spectroscopy study of composite coating created by a new method of active screen plasma nitriding on pure aluminum". *Surface and Coatings Technology*, 393, 125820, 2020. <https://doi.org/10.1016/j.surfcoat.2020.125820>
- [27] Taherkhani K, Soltanieh M. "Investigation of nanomechanical and adhesion behavior for AlN coating and AlN/Fe₂₋₃N composite coatings created by active screen plasma nitriding on Al 1050". *Journal of Alloys and Compounds*, 783, 113-127, 2019.
- [28] Vissutipitukul P, Aizawa T. "Wear of plasma-nitrided aluminum alloys". *Wear*, 259, 482-489, 2005.
- [29] Mohamed A, El-Madhoun Y, Bassim M N. "The effect of tempering on low cycle fatigue behavior of Al-2024". *Journal of Materials Processing Technology*, 162-163, 362-366, 2005.
- [30] Panigrahi S K, Jayaganthan R. "Effect of annealing on thermal stability, precipitate evolution, and mechanical properties of cryorolled Al 7075 alloy". *Metallurgical and Materials Transactions A*, 42, 3208-3217, 2011.
- [31] Sert Y, Küçükömeroğlu T, Efeoğlu İ. "Investigating the structure, adhesion and tribological properties of Al and Zr-doped TiN coatings with various substrate bias voltage and working pressure". *Proceedings of the Institution of Mechanical Engineers, Part J: Journal of Engineering Tribology*, 235(6), 1190-1202, 2021.
- [32] Kara L, Gahramanzade Asl H, Karadayı Ö. "The effect of TiN, TiAlN, CrAlN, and TiAlN/TiAlN coatings on the wear properties of AISI H13 steel at room temperature". *Surface Review and Letters*, 26(9), 1-14, 2019.
- [33] Gahramazadeh Asl H. "Investigation of friction and wear performance on oxidized Ti6Al4V alloy at different temperatures by plasma oxidation method under ambient air and vacuum conditions". *Vacuum*, 180, 109578, 2020. <https://doi.org/10.1016/j.vacuum.2020.109578>
- [34] Niu M, Zhang X, Chen J, Yang X. "Friction and wear properties of ni₃si alloy under different vacuum conditions". *Vacuum*, 161, 443-449, 2019.
- [35] Kovacı H, Baran Ö, Yetim A F, Bozkurt, Y B, Kara L, Çelik A. "The friction and wear performance of DLC coatings deposited on plasma nitrided AISI 4140 steel by magnetron sputtering under air and vacuum conditions". *Surface and Coatings Technology*, 349, 969-979, 2018.
- [36] Yetim A F. "Investigation of wear behavior of titanium oxide films, produced by anodic oxidation, on commercially pure titanium in vacuum conditions". *Surface and Coatings Technology*, 205(6), 1757-1763, 2010.
- [37] Küçükömeroğlu T, Kara L. "The friction and wear properties of CuZn₃₉Pb₃ alloys under atmospheric and vacuum conditions". *Wear*, 309(1-2), 21-28, 2014.
- [38] Raj A, Kailas S V. "Evolution of wear debris morphology during dry sliding of Ti-6Al-4V against SS316L under ambient and vacuum conditions". *Wear*, 456-457, 203378, 2020.
- [39] Gaard A, Krakhmalev P, Bergström, J. "Influence of tool steel microstructure on origin of galling initiation and wear mechanisms under dry sliding a carbon steel sheet". *Wear*, 267(1-4), 387-393, 2009.
- [40] Pujante J, Pelcastre L, Vilaseca M, Casellas D, Prakash B. "Investigations into wear and galling mechanism of aluminium alloy-tool steel tribopair at different temperatures". *Wear*, 308(1-2), 193-198, 2013.